buildings

MDPI

Article

Solar Energy-Driven Hardening of High-Performance Concrete Using THACs and Composite Binders

Aizhan Utkelbaeva [1], Kinga Korniejenko [2,*], Lyazat Aruova [3], Kamalbek Baitasov [1] and Assel Jexembayeva [4]

[1] Institute of Engineering and Technology, Kyzylorda State University, 29A Ayteke Bi Str., Kyzylorda 120000, Kazakhstan; aizhan85str@mail.ru (A.U.); kbaitasov@mail.ru (K.B.)
[2] Faculty of Materials Engineering and Physics, Cracow University of Technology, 37 Jana Pawła II Str., 31864 Cracow, Poland
[3] Faculty of Architecture and Civil Engineering, Gumilyov Eurasian National University, 13 Kazhymukan Str., r205, Astana 010008, Kazakhstan; ecoeducation@mail.ru
[4] Innovation Development Department, Gumilyov Eurasian National University, 13 Kazhymukan Str., r205, Astana 010008, Kazakhstan; dzheksembayeva_ae@mail.ru
* Correspondence: kinga.korniejenko@pk.edu.pl; Tel.: +48-609974988

Abstract

This research was motivated by the urgent need to address resource shortages and high energy costs in concrete production by replacing an energy-intensive traditional curing method with a new, more sustainable solution. By exploring solar heat treatment with composite binders and THACs, the study aimed to develop sustainable, cost-effective alternatives that harness renewable energy sources and optimize natural cement hydration processes for accelerated hardening. This article explores the potential application of solar energy in the production of precast concrete products using a composite binder. The effectiveness of the composite binder in solar thermal treatment of concrete using translucent heat-accumulating coatings is tested. The results of laboratory studies are presented, and the feasibility of using concrete based on composite binder at the laboratory scale for the production of concrete and reinforced concrete products, both with steaming and with solar thermal treatment, is established. The study of the structural features and basic physical and mechanical properties of hardened concrete under various conditions indicates that, under the investigated laboratory conditions, solar-thermally treated concrete exhibits physical and mechanical properties comparable to those of normally cured concrete. Laboratory studies confirmed the effectiveness of both steaming and solar heat treatment methods under controlled experimental conditions. Within the scope of the performed laboratory tests, the structure and properties of these concretes were comparable to those of normally cured concretes and, in several aspects, superior to those obtained under conventional steam curing regimes, which indicates the effectiveness of the described method, not only from the point of view of significant savings in fuel and energy resources. When producing products based on composite binders using solar thermal treatment, the consumption of the clinker portion of the binder is reduced by 50% (composition of the composite binder itself) and the consumption of conventional fuel during heat and moisture treatment is reduced by 70–100 kg per 1 m^3 of concrete (reflecting process-level comparisons), which is of significant value for external energy demand. These findings confirm the technical feasibility and environmental advantages of the proposed method at the laboratory scale and highlight its potential for broader industrial application in precast concrete production.

Check for updates

Academic Editor: Chi Yan Tso

Received: 17 March 2026
Revised: 15 April 2026
Accepted: 23 April 2026
Published: 26 April 2026

Copyright: © 2026 by the authors. Licensee MDPI, Basel, Switzerland. This article is an open access article distributed under the terms and conditions of the Creative Commons Attribution (CC BY) license.

Keywords: solar energy; solar heat treatment; composite binder; concrete; translucent heat-accumulating coatings; strength

1. Introduction

Despite extensive research into novel materials, traditional mineral binders such as Portland cement, lime, and gypsum, along with their variants, remain widely used in construction [1,2]. Since the mid-20th century, composite binders derived from these traditional materials—achieved through mixing or co-grinding with various additives—have been developed and integrated into industrial production [3,4]. These conventional binders dominate due to their proven strength, cost-effectiveness, and versatility in applications from residential to infrastructure projects. The global construction materials market, valued at USD 929.8 billion in 2025, underscores concrete's (cement-based) leadership at 26% revenue share amid ongoing urbanization [5]. Recent reviews collating conventional (water, steam/autoclave) and advanced curing routes (electric/microwave, carbonation) show that steam/autoclave reliably boosts early strength, but at the cost of higher energy demand and, if regimes are not carefully tuned, there are potential penalties in transport properties and long-term durability; alternative routes can cut energy but often lack factory-ready control and metrics [6,7].

As is known, there are two groups of mineral binders: air- and hydraulically hardened binders [8]. Depending on their efficiency and durability, they have a certain place in construction, but often there is a need to combine their various properties. For example, sometimes it is necessary to quickly harden concrete at a certain time to acquire the required properties. In the factory production of reinforced concrete products, there is a need to reduce the time of heat and moisture treatment. In monolithic construction, it is necessary to ensure the hardening and strength of concrete at negative and low positive temperatures. It is not always possible to solve these problems with the help of known mineral binders, so there is a need to create new progressive binders that meet the requirements of the time [8,9].

One of the solutions in this direction is the development of composite binders [10]. Composite binders are usually obtained on the basis of traditional binders and special additives that regulate certain of their properties. In composite binders, which represent a complex system, each element performs its inherent functions. The elements in the system are selected in order to ensure the expediency of the entire system. A change in a single element or the replacement of one element with another causes changes in the properties of the entire system, which shows the interconnection of the elements of the system with each other. Therefore, the correct selection of the elements of the system, taking into account their properties and contribution to the overall structure of the system, is important [11,12].

A composite binder consisting of a mixture of Portland cement, lime and mineral additive deserves careful study and introduction into production [13]. The binder is obtained by joint grinding of components, both at cement plants and at reinforced concrete plants. The fineness of grinding is 4000–5000 cm^2/g, the normal density is 34–37%, the beginning of setting is 40–50 min, and the end is 1 h 25 min–1 h 45 min. During the hardening of the binder, there is an accelerated increase in strength both under normal conditions and during steaming. This is an effective cement that makes it possible to abandon the usual heat and moisture treatment of concrete and reinforced concrete products [14,15].

Parallel progress has been observed in the area of composite and low-carbon binders, where waste-derived mineral components and clinker-reduced systems are increasingly used to improve sustainability and reduce the embodied energy of concrete [16,17]. These

developments underline the relevance of integrating alternative binders with energy-efficient curing technologies.

Accelerated curing methods remain an important industrial need, yet traditional thermal regimes such as steaming are energy-intensive and may induce microstructural drawbacks when not properly controlled. Consequently, recent research has focused on hybrid or solar-assisted curing: solutions capable of reducing external energy demand while maintaining mechanical performance [18].

In the context of industrialization of construction production, the construction of engineering structures using intensive technology, the implementation of an energy-saving policy in the practice of construction, and the use of solar energy in the technology of concrete works acquire economic significance [19,20]. The fundamental evidential role of the use of solar energy for concrete hardening should be attributed primarily to energy, technological and technical problems, the solution of which determines the expediency of involving a new energy source in the energy balance of construction industry enterprises [21]. The use of solar energy in the technology of concrete works is attractive due to its savings in traditional fuels, as well as the absence of harmful emissions into the environment [22,23].

The problem of using solar energy in the technology of concrete works is associated with deep experimental research and the creation of technically and economically effective simple devices and installations. An effective way to use solar energy with an efficiency of 0.6–0.75 for heat treatment of concrete is solar heat treatment [18]. Case studies (solar dryers/greenhouses or solar-heated steam) confirm feasibility and early-age strength gains in warm/arid climates, yet typically report limited control of boundary conditions (T/RH gradients) and scarce LCA-ready, plant-comparable energy metrics (kg FOE·m^{-3}/m^3 NG·m^{-3}) [24–26].

The study of the use of solar energy in accelerating the hardening of concrete according to the literature, the generalization of experience, and the analysis of the operation of solar chambers and solar installations, as well as preliminary studies, made it possible to put forward the concept of the possibility and efficiency of accelerating the hardening of concrete of prefabricated products directly in molds due to solar energy. The essence of this approach lies in the fact that each product heated in the mold is considered as a kind of solar receiver, while the hardening concrete itself is the absorbing and accumulating element of the receiver, the metal mold is its body, and the only additional element—the cover according to specially calculated lighting and thermal parameters—plays the role of a transparent coating. Thus, an ordinary, typical metal mold equipped with a solar cap turns into a new type of gel equipment called helioform [27–30].

Direct use of solar radiation with the natural density of the radiant flux and its conversion into thermal energy on the surface of the heated concrete is implemented in the translucent heat-accumulating coatings, which makes it possible to reduce labor and material resources. This kind of technology has been developed for the production of prefabricated reinforced concrete products in helioforms with translucent heat-accumulating coatings (THACs) [21,31,32]. Direct solar radiation aggravates plastic shrinkage via elevated evaporation/temperature unless the surface microclimate is controlled—underscoring the need for a moisture-retentive interlayer such as THAC to stabilize RH and gradients [6,33].

Concrete hardening under THACs is characterized by a structure similar to the structure of normal-hardening concretes, which is also confirmed by the results of studies of their frost resistance and water tightness. The THAC significantly changes the temperature modes of concrete hardening both at the stage of its heating by a radiation flux, and when the products are aged at night. At the stage of heating the products, the design of the THAC should ensure the maximum use of direct and diffuse solar radiation for an intensive increase in the temperature of the surface of the product. In the absence of a radiation flux,

the same structure should create conditions for thermos storage of heated concrete with slow cooling of the product. The versatility of the THAC design is necessary to reduce labor costs when servicing heliforms, to abandon the use of additional heat-insulating coatings at night and to guarantee high physical and mechanical characteristics of concrete after heat and humidity treatment [34,35].

Despite promising energy-saving potential, existing solar-curing technologies are limited by fluctuating climatic conditions, incomplete control of heat and moisture transfer, non-uniform temperature fields, and inadequate protection against surface drying, all of which reduce curing reliability in practice [36,37]. To bridge this gap, we propose a THAC-integrated curing approach that moderates environmental variability, enhances the stability of heat–moisture exchange, and enables more predictable hydration kinetics.

Addressing the literature gap, the article operationalizes solar-assisted curing as a controlled process by combining a THAC moisture-retentive boundary (near-saturated interlayer, soft ΔT) with a clinker-reduced binder, and quantitative, factory-ready energy accounting derived from measured steam demand and efficiency envelopes—closing gaps in (i) process-level control, (ii) integrated materials–process quantification within one dataset, and (iii) transparent, plant-comparable energy metrics.

The purpose of the study is to study the properties of concrete based on a composite binder when using solar THAC. The authors have studied the possibility of using a composite binder for the production of products using concrete solar technology. The combination of composite binder and solar heat treatment of concrete can provide significant energy savings [15]. The dependence of the kinetics of heating and hardening of concrete in helioform on W/C (water/cement), the consistency of the concrete mixture and other technological factors, the kinetics of concrete strength growth, and the effect of solar heating on the increase in the strength of concrete of various consistencies was investigated. A study of the effect of the type of filler, the initial temperature of the concrete mixture, various chemical impurities and other technological factors on the processes of structure formation during solar thermal treatment using THAC and other methods of accelerated concrete hardening was also carried out.

This study advances solar-driven curing by quantifying the energy–hydration coupling in THAC-based regimes using a clinker-reduced composite binder, demonstrating that up to ~45–50% of the early-age heat input can be provided by cement exothermy under low-intensity solar flux. In a side-by-side evaluation of THAC, steaming, and normal curing, we map strength development, maturity, porosity, and frost resistance, demonstrating performance parity of THAC-cured concretes with normally cured counterparts while simultaneously enabling a 50% reduction in clinker content and 70–100 kg fuel savings per m^3 at the production scale. This integrated materials–process route clarifies how THAC boundary conditions unlock efficient hydration heat utilization and provides a practical, scalable pathway for low-carbon accelerated hardening. In particular, the novelty aspects are:

- Process-level integration, not component-level trials. The study systematically combines a clinker-reduced composite binder with a translucent heat-accumulating coating (THAC), treating the curing interface (temperature, moisture retention, and radiative flux) as an active process variable rather than a passive cover. This converts solar curing from an empirical practice into a controllable curing regime.
- Unified experimental framework linking performance and energy metrics (end-to-end quantification in one dataset). Mechanical properties (early-age and 28-day strength), maturity index, porosity, and frost resistance are evaluated together with process-level energy accounting. This avoids cross-study extrapolation and enables a direct link between curing method, microstructural quality, and avoided fuel demand.

- Industry-oriented quantification of energy savings. The traceable fuel saving of 75–100 kg FOE m^{-3} (≈35 m^3 NG m^{-3}) derived from measured steam was calculated based on demand and efficiency envelopes, and scaled to national production, meeting LCA transparency. The methodology translates laboratory curing results into factory-comparable energy metrics (avoided steam demand, fuel mass and volume equivalents per m^3), providing a transparent and transferable basis for industrial assessment rather than a purely qualitative sustainability claim.
- Explicit control and measurement of the thermal–moisture environment. It was shown that THAC conditions harvest hydration heat (≈45–50% of early input) while avoiding steep gradients typical for steam cycles, thereby enabling clinker reduction (−50%) without performance loss. Unlike many prior studies on solar or hybrid curing, the methodology tracks temperature fields, relative humidity in the interlayer, and maturity development under stabilized boundary conditions, allowing direct comparison with normal curing and steam curing within the same experimental framework.

2. Materials and Methods

Portland cement M400, crushed granite of fraction 5–20 mm and quartz sand with a particle size of Mkr = 3.4 were used in this experiment. The research was carried out according to standard regulatory documents and methods: GOST 18105-2018 [38] and GOST 10060-2012 [39].

The experiments used a composite binder consisting of Portland cement M400 (50% by weight), quicklime (20%), and thermal power plant ash (30%). The binder components were jointly ground to ensure homogeneity and stable reactivity.

As is well established, Portland cement is produced by grinding Portland cement clinker, which therefore represents the dominant source of embodied energy and emissions in the binder system. In the applied composite binder, 50–70% of the Portland cement is replaced by lime and thermal power plant ash, resulting in a corresponding reduction in clinker consumption. In the specific mix design used in this study, the Portland cement content was limited to 50 wt.%, while the remaining fraction was composed of lime and ash. This compositional approach provides a quantified basis for the reported reduction in clinker content, enabling reproducibility and comparison with other low-clinker binder systems.

The composite binder consisted of three solid components combined in clearly defined mass proportions. The binder was formulated using Portland cement, lime, and an acidic active mineral additive. In the representative composition used in this study, the proportions by weight were as follows: Portland cement—50 wt.%, lime—20 wt.%, and acidic active mineral additive—30 wt.%.

All components were jointly ground in a ball mill until a specific surface area of approximately 5100 cm^2/g was achieved, ensuring homogeneous dispersion of the constituents and reproducible reactivity of the binder. The normal consistency of the resulting composite binder paste was in the range of 0.33–0.37, as determined by standard testing methods.

Solar thermal treatment was carried out using translucent heat-accumulating coatings (THAC). The standard configuration included a layer of translucent material, typically polyethylene film, mounted on a rigid metal or plastic frame with stretched films. An air gap was intentionally created between the freshly cast concrete surface and the translucent coating, forming a moisture-retentive and thermally moderated interlayer. This configuration allowed controlled solar heat transfer while limiting evaporative cooling and plastic shrinkage during early-age hardening.

The overall scheme for the investigation is presented in Figure 1.

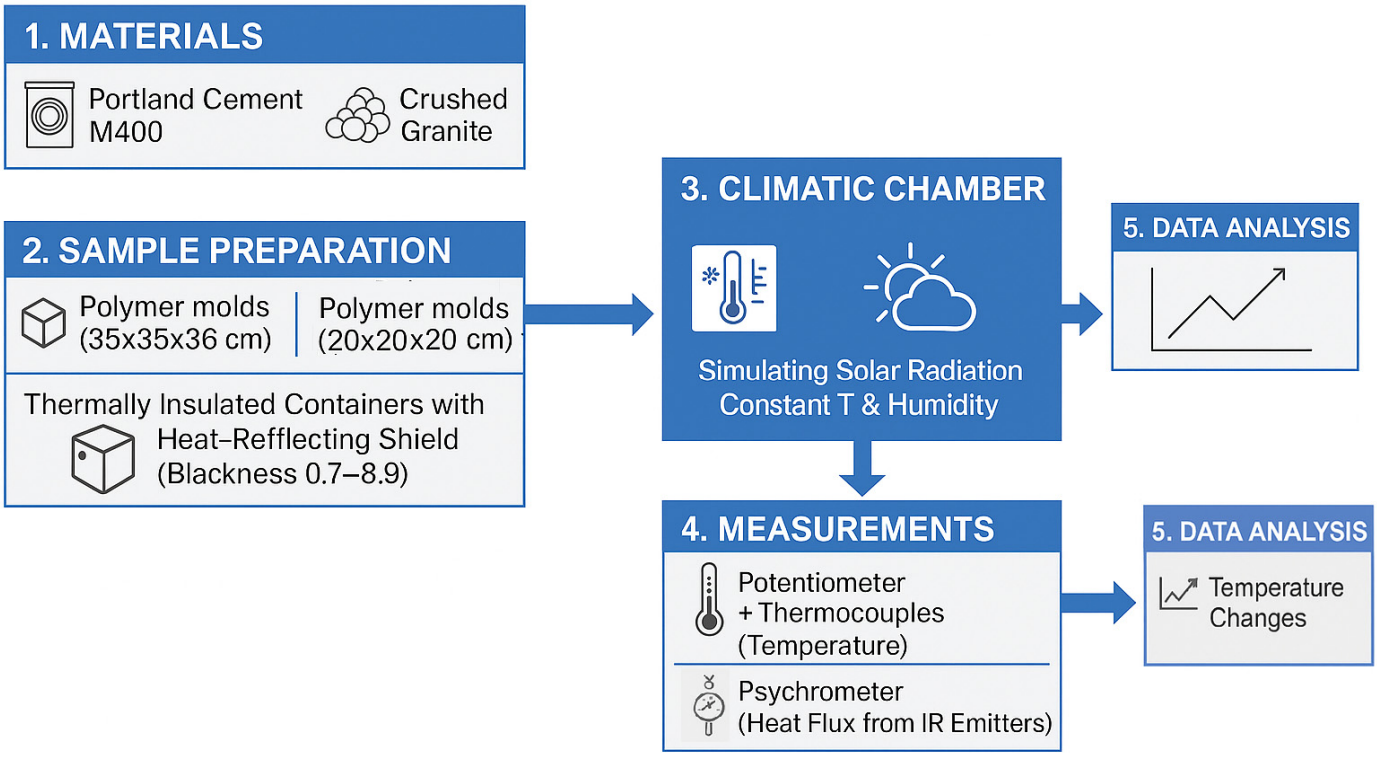


Figure 1. Experimental program and curing regimes considered in the study.

Under natural conditions, solar radiation falling on the Earth's surface undergoes changes and is determined by the physical state of the atmosphere. Changes in temperature and humidity during the day require the solution of many thermophysical problems when performing experimental work. Therefore, in order to obtain reliable experimental data, research should be carried out in conditions of constant temperature and humidity. To conduct experimental studies, a climatic chamber (Komek LLC., Kyzylorda, Kazakhstan) was used, which simulates the conditions of a hot, dry climate and the effects of solar radiation on a horizontal surface.

A 1.5 × 2.2 × 2.2 m climate chamber was used for the experimental studies. It simulates hot, dry climate conditions and solar radiation falling on a horizontal surface. The walls, coating, and floor of the chamber are thermally insulated. To reflect radiation, the interior walls of the chamber are lined with a metallized shell.

The study of the temperature field in concrete and the air temperature in solar devices was carried out on an automatic electronic potentiometer of the KSP-4 type (Manometer Plant, Moscow, Russia) using a Chromel-Copel metal-based thermocouple that uses Chromel (nickel–chromium alloy) for the positive leg and Copel (copper–nickel alloy) for the negative leg.

The humidity of the air was monitored and recorded using an automatic psychrometer (JSC Steklopribor, Zavodske, Ukraine).

Through the observation window in the chamber, the readings of the instruments were carried out and the state of infrared emitters (Elektronagrev LLC, Moscow, Russia) moving along the guides fixed on the wall was monitored.

The design of measuring the heat fluxes of infrared emitters was carried out according to the method of N.N. Danilov using a radiometer [40].

Optimization of the translucent coating design was carried out through research into the lighting and performance characteristics of translucent materials and determining the number of coating layers. The initial selection criteria for translucent materials included: solar transmittance and the transmittance of rays emitted by heated concrete, durability,

and cost. The coatings were constructed using wooden or plastic frames with translucent materials sandwiched between them. The bottom frame of the roof, located on a block form, was glued to it with epoxy adhesive. The remaining frames were connected to the bottom frame and to each other with screws. Based on their performance, as assessed by the thermal conductivity of concrete, the translucent materials in translucent coating were arranged in the following order: glass, polyvinyl chloride film, and polyethylene film. Structurally, the translucent coating is most conveniently designed as a special insert in the solar coating body.

To study the temperature field of hardening concrete, special thermally insulated containers in the form of flat collectors were developed. The body receives heat in a semi-confined space, the degree of blackness of which is 0.7–0.9 for hardening concrete. The concrete mixture was placed in novotext molds (polymeric) measuring 35 × 35 × 36 and 20 × 20 × 20 cm and placed in a thermally insulated container, the inner part of which was covered with a heat-reflecting shield.

A statistical analysis of the experimental results was carried out using a full factorial experimental design, which enabled quantitative evaluation of the influence of the main factors and their interactions on the studied properties. The experimental data were processed using multiple regression analysis, and the relationship between the optimization parameters and the influencing factors was described by a second-order polynomial regression model of the following general form:

$$y = b_0 + \sum_{i=1}^{k} b_i x_i + \sum_{i=1}^{k} b_{ii} x_i^2 + \sum_{i=1}^{k} \sum_{j=1}^{k} b_{ij} x_i x_j \quad (1)$$

where y represents the response functions, namely the ultimate compressive strength after 28 days of normal curing, as well as the compressive strength after 4 h and 28 days of steam curing, and x_1 and x_2 correspond to the lime content and ash content in the lime–ash Portland cement, respectively.

Based on the experimental plan, the regression coefficients were calculated, and statistically significant models describing the behavior of the studied optimization parameters were obtained. The regression models allowed for assessment of the individual effects of the factors, their quadratic terms, and their interaction, providing a statistically grounded basis for determining the optimal binder composition. This approach ensures both the reliability of the results and the reproducibility of the study

3. Results

Due to the fact that the surface of hardening concrete is characterized by a sufficiently high coefficient of absorption of sunlight due to the transition to the heat of short-wave solar radiation, the products gradually heat up and the water mixed with concrete begins to evaporate intensively. Dehydration leads to rather large plastic shrinkage, which destroys the formed structure of concrete, significantly worsens its basic physical and mechanical properties and causes the formation of cracks.

From the point of view of heat engineering, external mass transfer is the cause of a decrease in the temperature of concrete during the hardening of concrete heated by sunlight. In hardening concrete, undesirable processes of cooling of the surface layers of concrete during evaporation, affecting the service life of concrete, are observed under the influence of solar radiation during the manufacture of the product in landfill conditions, and in heat treatments, in which the unshaped upper surface of the product is exposed. The same processes can occur in solar chambers, in which the volume of free air in the chambers absorbs evaporating, superheated moisture vapors from concrete.

Therefore, the use of solar THAC provides, first of all, intensive mass transfer processes and blocking of plastic shrinkage in hardening concrete, serving as an effective means of concrete care not only under conditions of solar radiation, but also under extreme environmental parameters characteristic of a dry hot climate. An indicator of complete moisture saturation of the air gap between the surface of the product and the THAC is the formation of condensate droplets on the lower surface of the coating, which indicates that the relative humidity of the air in the gap is close to 100% and negative physical processes in the heated concrete are neutralized.

It is instructive to consider the dependence of the kinetics of heating and hardening of concrete in helioform on W/C, the consistency of the concrete mixture and other technological factors. The relevant studies were carried out in natural conditions of a dry, hot climate. Concrete samples were hardened in molds with an individual coating of THAC am, placed on a special laboratory stand, the side surfaces of which were isolated from the environment.

Absorption of solar radiation of concrete and its heat exchange with the environment were carried out mainly due to the gap between the upper surface of the samples and the THAC. Heating and kinetics of increasing the strength of concrete were studied on standard samples with dimensions of 15 × 15 × 15 cm and on standard blocks with dimensions of 40 × 40 × 15 cm, reflecting the hardening conditions of a particular product [16]. The kinetics of heating were studied using a Chromel-Copel thermocouple and an automatic KSP-4 potentiometer. In the experiments, we used an anisotropic binder based on Portland cement M400, crushed granite of fraction 5–20 mm and quartz sand with a particle size of Mkr = 2.5 and Mkr = 3.4.

A reduction in W/C leads to higher internal temperatures during solar thermal treatment, primarily due to the stronger exothermic response of the binder. This is reflected in the maturity development: over a 24 h period, concretes with W/C = 0.80, 0.60, and 0.40 reached approximately 910, 957, and 1052 °C·h, respectively. These results demonstrate that at lower w/c ratios, the hydration heat contributes substantially to the temperature rise, increasingly dominating the thermal regime. When combined with the low-intensity external heat flux provided by THAC, the internal hydration heat accounts for 45–50% or more of the total energy absorbed by the concrete at early age. This synergy between solar input and hydration kinetics explains the accelerated maturity and improved early-age strength observed under THAC [32].

Table 1 shows data on the kinetics of concrete strength growth in standard samples with a size of 15 × 15 × 15 cm. According to them, when hardening under the THAC at W/C = 0.6–0.8, concretes of classes B15 and B22.5 showed a strength of 28 after 12 h—30%, and for $R_{28}^{H.T.}$ at W/C = 0.4, the index of concrete of class B30 was 37–44%. After 1 day, these $R_{28}^{H.T.}$ values were 38–45 and 51–58%, respectively; after 2 days, they were 50–61 and 64–70%. The first $R_{28}^{H.T.}$ values in these data refer to THAC based on polyethylene film, and the second to THAC based on PVC(B).

Table 1 also shows that the efficiency of solar thermal treatment increases slightly with an increase in W/C compared to normal hardening. If W/C = 0.4–0.6, then after 12 h, the strength of the heliothermally treated concrete exceeds the strength of normal hardening concrete by 4–4.1 times for PVC(B)-based THAC and 3.42–3.52 times for polyethylene-based THAC. In a daily period, these indicators amounted to 2–2.1 and 1.74–1.83 times, respectively, and in 2 days, 1.3–1.65 and 1.3–1.4 times. At W/C = 0.8, the indicators are 4.4 and 3.9; 2.5 and 2.24; and 1.68 and 1.57 times, respectively. This is due to the fact that concretes with low W/C are characterized by a relatively rapid acceptance of initial strength even at normal hardening temperatures.

Table 1. Dependence of the strength of concrete hardened under the THAC on W/C.

Concrete Hardening Condition	W/C	Compressive Strength, MPa/% $R_{28}^{H.T}$			
		12 h	1 Day	2 Days	28 Nights
2 days under THAC, then in natural conditions; film—PVC	0.4	19.8/43.6	25.2/58.4	30.4/69.2	39.6/92.1
	0.6	9.1/30.5	12.5/41.3	18.2/60.9	28.1/94.4
	0.8	5.2/26.4	8.2/44.8	10.1/57.4	19.0/103.2
2 days under THAC, then in natural conditions; film—polyethylene	0.4	16.4/37.8	22.4/50.5	28.5/64.7	40.5/90.4
	0.6	8.1/25.2	11.1/38.5	15.2/51.7	26.7/93.5
	0.8	4.7/24.3	7.7/42.1	10.4/51.5	18.2/100.4
Hardening in natural conditions	0.4	4.7/11.9	12.5/31.1	21.4/49.6	21.7/49.6
	0.6	2.3/7.4	6.3/20.2	10.5/36.5	28.6/100
	0.8	1.2/6.25	3.3/15.9	6.2/31.8	18.2/100

Note: Slump = 20 mm.

It is known that the more rigid the concrete mixture to be laid, the more intensive the initial hardening of the concrete. On the other hand, as the mixture stiffness increases, both the peak temperature reached during solar heating and the corresponding maturity index (°C·h) accumulated over the daily curing period decrease slightly. This affects the growth of concrete strength at the initial stage of hardening; therefore, interest was aroused by studies of the effect of solar heating on the growth of the strength of concrete of various consistencies.

The studies used concrete with W/C = 0.54 with a water content of 211 L/m^3 (slump = 60–70 mm), 190 L/m^3 (slump = 20–30 mm) and 160 L/m^3 (F = 30–40 s), mixture hardness and seconds.

Indicators of concrete strength (W/C = 0.6), depending on the consistency of the mixture and the period of concrete hardening, are given in Table 2.

Table 2. Kinetics of concrete strength growth at different consistencies of concrete mixture and solar heat treatment.

Concrete Hardening Condition	Consistency of Concrete Mixture, Slump	Compressive Strength of Concrete, MPa/% $R_{28}^{H.T}$		
		0.5 Day	1 Day	28 Days
Experimental (THAC-assisted solar curing)	60–70 mm	6.8/19.6	11.2/35.2	31.8/100.5
Normal curing (reference)		1.68/5.05	6.18/17.8	32.4/100
Experimental (THAC-assisted solar curing)	20–30 mm	8.41/24.5	12.4/39.5	31.4/100.2
Normal curing (reference)		2.39/7.25	5.98/18.8	32.0/100

Note: Experimental hardening: 1 day under the THAC, 3 days under the film in the air, then in a dry hot climate without care.

As can be seen from the table, the maturity index (°C·h) of concrete hardened under the THAC is slightly reduced, although at constant W/C, the strength of concrete increases significantly for more rigid mixtures.

The study of the growth of concrete strength in cube samples (15 × 15 × 15 cm) during solar heat treatment made it possible to identify a dependence of concrete strength on W/C. According to this dependence, the daily strength of concrete of class B15 made on a composite binder based on Portland cement M400 and solar thermoworked under the

THAC in hot climate conditions is 42–45% $R_{28}^{H.T}$ and the daily strength of concrete class B30 is 52–58% $R_{28}^{H.T}$.

A comparative analysis of the heating of concrete by various methods of care in a dry hot climate and increasing its strength showed that the existing methods that provide wet hardening conditions mainly protect the concrete from the effects of solar radiation. The use of ready-made polymer films, which are laid directly into concrete, can be attributed to the methods of accelerating the curing of concrete by using solar energy (Table 3).

Table 3. Maturity and strength of concrete samples under different maintenance methods.

Condition for Concrete Care	Concrete Maturity at the Age of 1 Day, °C·h	Tensile Strength of Concrete of Class B22.5 at the Age of 1 Day, %
Normal hardening	523	100
Permanently moistened mat coating	638	108.2
Use of liquefied bitumen	636	112.9
Concrete-coating polyethylene film	-	140.5
Application of THAC with polyethylene film	792	166.4

However, this method does not have any fundamental advantages over other approaches to care, since the strength of the concrete when it is used is relatively low (30–35%) and this $R_{28}^{H.T}$ does not provide a daily cycle of reinforced concrete production, not to mention other disadvantages. At the same time, the use of THAC makes it possible to obtain a strength that exceeds the strength of normal hardening concrete by 1.7 and 2 times in a daily time and to obtain, depending on the brand of concrete, 40–60% $R_{28}^{H.T}$.

A study of the effect of the type of filler, the initial temperature of the concrete mixture, various chemical impurities and other technological factors on the processes of structure formation during solar thermal treatment using the THAC was also carried out. Results of the study of temperature fields of products and hardening samples with a thickness of 300–400 mm showed that their heating under the THAC in helioforms is carried out according to soft modes, under which the rate of increase in the concrete temperature is 5–7 °C/h, duration of conditional isothermal content at a maximum temperature of 60–70 °C is 5–7 h, and cooling to a temperature of 35–50° depends on the weight of the product, the brand of concrete, the ambient temperature, etc., and passes at a speed of 1.5–2.5 °C/h.

Such modes create favorable conditions for concrete hardening, which should have a positive effect on the formation of the structure and properties of concrete. The structure and basic physical and mechanical properties of concretes hardened in helioforms under the THAC were compared with steamed concretes in accordance with the traditional modes and normally hardened concretes.

In the experiments, a Portland cement-based composite binder based on Portland cement M400, crushed granite of fraction 5–20 mm and quartz sand with a particle size of Mkr = 3.4 was used. The composition of the tested concrete was 1:2.52:3.4; W/C = 0.6; cone cettling slump = 10–30 mm. Cube samples with an edge size of 15 cm were prepared in three batches and hardened under different conditions.

Samples of the first series were hardened under the conditions of the city of Kyzylorda under the THAC for 20–22 h; then, after removal from the molds, they were hardened for two days under polyethylene film, and then placed in natural conditions. The samples of

the second batch were steamed at a temperature of 85 °C in accordance with the regime of 2 + 3 + 6 + 3 h and removed from the molds one day after preparation. Then, they were stored in a Normal Curing Chamber for 28 days.

The characteristics of macro- and microstructures of concretes, including total and differential macroporosity, as well as the maturity index of cement, were studied.

Macro studies were carried out on fragments and flat surfaces of the specimens, and micro studies were carried out on transparent and polished sections made from these specimens. Pore sizes (in the range of 1–800 μm), differential and total porosity, and the degree of hydration were determined under a microscope using an eye grid and a ruler. In contrast to steamed concretes with a loose and coarse-pored structure, concretes hardened under the THAC are characterized by low macroporosity and large size of crushing pores by dimensions (Table 4).

Table 4. Structural characteristics of concrete.

No Series	Size and Number of Pores Relative to Total Porosity, %									Total Porosity Mortar Parts, %
	1–15	20–30	40–50	60	75	80–150	160–300	350–450	600	
1	1	13	12	25	24	10	11	1	3	3.0
2	2	1	4	6	6	32	32	5	12	3.78
3	-	2	7	15	21	23	20	6	6	3.49

Note: Series 1 (THAC), Series 2 (steam), Series 3 (normal).

Concrete hardened under THAC shows lower macroporosity, which is consistent with the observed increase in compressive strength and the improved resistance to freeze–thaw cycles. In terms of the main structural characteristics, concretes that hardened under normal conditions and concretes treated with solar heat treatment are similar. They are distinguished by the dense structure of cement stone and the mortar part with evenly distributed small pores of a regular round shape.

Similar conclusions were made based on the results of studies of the frost resistance of concrete, which indirectly characterize the features of the concrete structure (Table 5). It can be seen that when tested for up to 300 cycles, the difference in the frost resistance of concretes treated with solar heat treatment under the THAC and hardened under normal conditions is insignificant. The comparable frost-resistance values after 300 freeze–thaw cycles can be attributed to the refined pore structure and reduced large-pore volume produced by the THAC-assisted curing regime.

Table 5. Frost resistance of concrete.

No Series	Compressive Strength of Concrete After Cycles of Alternate Freezing and Thawing, MPa			
	0	100	200	300
1	30.1	30.5	32.5	33.7
2	26.8	33.7	33.8	31.8
3	29.7	31.4	36.5	36.5

The strength development, pore structure characteristics, and frost resistance observed in this study are closely interrelated and reflect a common microstructural mechanism governed by the curing regime. The moderated thermal conditions provided by THAC-

assisted solar curing promote a more uniform hydration process, resulting in a denser cement matrix with a reduced proportion of large macropores.

This refined pore structure contributes directly to the improved compressive strength by limiting stress concentration sites and enhancing load transfer within the cementitious matrix. At the same time, the reduced connectivity and size of capillary pores play a key role in limiting water ingress and internal ice formation, which explains the frost-resistance performance comparable to that of normally cured concrete. The consistency of strength, porosity distribution, and freeze–thaw resistance, therefore, indicates that THAC-assisted curing affects concrete performance through a unified microstructural refinement mechanism rather than through isolated property changes.

In steamed concrete, the speed of these processes slows down due to the formation of dense neoplasms around the cement grains at relatively high temperatures, which makes it difficult for moisture to penetrate into the grain. At the same time, the waterproofness of steamed concrete does not increase over time; it remains about 0.4 MPa due to significant destruction of its structure, the presence of a mortar part and the presence of micro and macro cracks, as well as other defects in the contact zone.

It should be noted that the studies used steamed concrete in a vapor-air environment at $\varphi \geq 95\%$. In addition, heat treatment of products at landfills and open shops of reinforced concrete plants in many cases is carried out by contact heating in open thermoforms, during which as a result of the intensive course of external and internal heat exchange processes, unfavorable conditions are created for the formation of a concrete structure, which leads to its premature cracking, excessive drying, deterioration of basic properties and a sharp decrease in durability. In this case, the advantages of solar heat treatment of products using THAC are the most obvious.

Storage of concrete in hot and dry weather without maintenance ensures the purchase of about 40% of concrete of class B22.5 (M300) $R_{28}^{H.T}$ in a day, but causes significant primary destruction of concrete and a loss of strength of more than 40% in a month. Therefore, in a dry, hot climate, such "solar heat treatment" of reinforced concrete is strictly prohibited. As noted above, the cubic strength of the heliothermally treated samples in the daily period depends on the value of the W/C and is 40. In addition, the cubic strength of concrete hardened under the THAC for a month usually does not differ much from the strength of concrete that hardened under normal conditions.

It is known that the modulus of elasticity of parboiled concrete at atmospheric pressure and temperatures up to 100 °C at the age of one month is about 10–15% less compared to the modulus of elasticity of concrete hardened under normal conditions. Since the concrete under the THAC heats up at low temperatures, it can be expected that its modulus of elasticity will be slightly higher than that of steamed concrete.

Figure 2 presents the compressive strength for the samples treated by different kinds of methods.

The studies were carried out on cube samples with a face size of 15 cm and prisms of 10 × 10 × 40 cm. The results given in Table 6 indicate that the prism strength, flexural tensile strength and elastic modulus of concretes hardened under the THAC are slightly higher in a month than in steamed concrete, which is explained by the softness of the solar heating mode.

Thus, the study of the structural features and basic physical and mechanical properties of hardened concretes under various conditions indicates the high quality of solar-heat-treated concretes. The structure and properties of these concretes are better than those of steamed concretes under traditional conditions, and are close to hardened concretes under normal conditions, which indicates the effectiveness of the described method not only from the point of view of significant savings in fuel and energy resources.

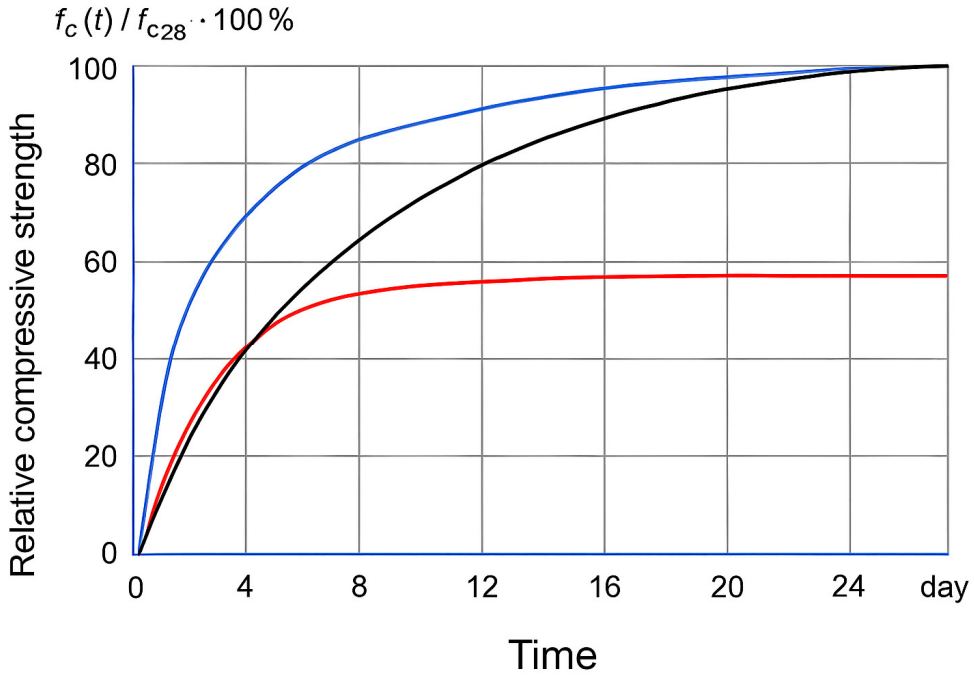


Figure 2. Normalized compressive strength development of concrete under different curing conditions: black line—hardening under normal conditions; red line—hardening in natural conditions of a dry, hot climate without maintenance; blue line—solar thermal treatment of concrete using the THAC, where $f_c(t)/f_{c28}$ 100% means strength gain at t days (%).

Table 6. Strength characteristics of concrete.

No Series	Cube		Rpr	R		E·103
	1 Day	28 Days	28 Days	1 Day	28 Days	
1	12.6/44.7	31.5/104.7	31.8/105.7	2.59/45.5	5.28/94.9	33.2/94.8
2	20.6/71.9	30.3/101.5	21.0/86.2	3.65/66.7	5.14/90.5	29.4/86.5
3	5.55/18.7	29.6/100.0	24.8/100.0	1.48/26.4	5.38/100.0	33.5/100.0

Note: Before the line MPa; After the line $R_{28}^{H.T.}$.

The experiments described above were carried out on a laboratory bench, mainly on standard samples of 15 × 15 × 15 cm.

4. Calculation of Energy Savings from Solar-Assisted Heat Curing

This chapter presents the calculation of the primary energy/fuel avoided by replacing conventional steam heat treatment of precast concrete with solar heat. The system boundary is factory curing only (no upstream raw materials, transport, or end-of-life). The functional unit is 1 m^3 of concrete; we then scale to the reported annual production volumes.

The calculation is based on the following process data: Factory steam curing uses 500 kg steam per 1 m^3 of concrete. One kilogram of steam supplies 600 kcal, and hence 1 m^3 requires 300,000 kcal of heat (Equation (2)). Equivalently, 300,000 kcal ≈ 1.255 GJ ≈ 349 kWh (Equation (3)). Steam demand is often expressed as natural-gas equivalent: the plant ratio is 35 m^3 natural gas (NG) per 1 m^3 of concrete (Equation (4)).

$$\text{Heat per 1 } m^3\text{: } Qc = 500 \text{ kg} \times 600 \text{ kcal/kg} = 300{,}000 \text{ kcal} \quad (2)$$

Unit conversions:

$$300{,}000 \text{ kcal} \times 4.186 \text{ kJ/kcal} = 1255.8 \text{ MJ}, 1255.8 \text{ MJ} \div 3.6 \text{ MJ/kWh} \approx 349 \text{ kWh} \quad (3)$$

$$\text{Plant gas factor: } 300{,}000 \text{ kcal} \Leftrightarrow 35 \text{ m}^3 \text{ NG} \quad (4)$$

Annual activity data are as follows: using solar technology, Kazakhstan produces 2,000,000 m^3 (spring–fall), 1,000,000 m^3 (winter), and 3,000,000 m^3 total.

Based on the data presented above the avoided energy (per m^3 and annually) was calculated. Per 1 m^3: 349 kWh and 35 m^3 NG are avoided. Annually,

- Spring–fall block: 2,000,000 m^3 × 35 m^3/m^3 = 70,000,000 m^3 NG avoided.
- Winter block: 1,000,000 m^3 × 35 m^3/m^3 = 35,000,000 m^3 NG avoided.

It gives a total 105,000,000 m^3 NG avoided, equivalent to 3,000,000 × 349 ≈ 1.05 TWh or 3.77 PJ of heat.

Using these data, it is possible to reach a mass-based fuel metric. The heat required for the concrete is Q_c = 300,000 kcal/m^3, but the fuel at the boiler must cover generation and distribution losses. Let η be the overall efficiency from fuel to delivered steam at the mold (combustion + boiler + piping + enclosure losses). In this case, the fuel energy input per 1 m^3 is given by

$$Q_{\text{fuel}}(t) = \frac{Q_c}{\eta} = \frac{300{,}000}{\eta} \text{ kcal/m}^3$$

Converting to kg of fuel depends on the lower heating value (LHV) of the fuel actually burned. The typical values for selected fuels are presented in Table 7.

Table 7. Fuel lower heating values (LHVs) and calculated fuel demand to provide 300,000 kcal per 1 m^3 of concrete (steam curing).

Fuel/Form	LHV (Basis)	LHV (Converted)	Sources
Heavy fuel oil	41.4 MJ/kg (LHV)	≈9900 kcal/kg	[41]
Gasoil/diesel	42.8 MJ/kg (LHV)	≈10,230 kcal/kg	[42]
Natural gas (NG)—mass basis	47.1 MJ/kg (LHV)	≈11,255 kcal/kg	[42]
Natural gas (NG)—volume basis	36.6 MJ/m^3 (LHV)	≈8750 kcal/m^3	[42]
Coal—anthracite/hard coal	33 MJ/kg (LHV, typical)	≈7890 kcal/kg	[43]

The table presents the lower heating values (LHVs) and calculated fuel requirements to deliver 300,000 kcal per cubic meter of concrete (steam curing). Fuel mass is computed as m = (300,000/η)/LHV, with η ∈ [0.30, 0.40] to represent boiler, distribution, and enclosure losses. The presented data allows us to present the following calculations:

Fuel oil (LHV ≈ 10,000 kcal/kg):

$$m_{\text{oil}} = \frac{300{,}000/\eta}{10{,}000} = \frac{30}{\eta} \text{ kg/m}^3$$

For η = 0.30–0.40 (typical of aging curing lines with distribution losses),

$$m_{\text{oil}} = 75\text{–}100 \text{ kg/m}^3.$$

Natural gas (LHV ≈ 11,255 kcal/kg as mass-based reference):

$$m_{\mathrm{NG}} = \frac{300{,}000/\eta}{11{,}255} \approx \frac{26.7}{\eta}\ \mathrm{kg/m^3}.$$

For η = 0.35, $m_{\mathrm{NG}} \approx 76.2\ \mathrm{kg/m^3}$.
Coal (LHV ≈ 7000 kcal/kg):

$$m_{\mathrm{coal}} = \frac{300{,}000/\eta}{7000} = \frac{42.9}{\eta}\ \mathrm{kg/m^3}.$$

For η = 0.35, $m_{\mathrm{coal}} \approx 123\ \mathrm{kg/m^3}$.

Under realistic overall efficiencies η = 0.30–0.40 for steam curing lines (accounting for boiler, flash/vent, distribution and enclosure losses), the avoided fuel mass spans ~70–100 $\mathrm{kg/m^3}$ when expressed as fuel oil equivalent (FOE) and ~70 $\mathrm{kg/m^3}$ for natural gas at η ≈ 0.35.

For transparency across unit systems, we additionally verify that the mass-based savings (75–100 kg $\mathrm{FOE/m^3}$) are consistent with the plant's volume-based metric (35 $\mathrm{m^3\ NG/m^3}$), showing numerical agreement under the same efficiency assumptions; this cross-check does not alter the result but confirms unit coherence. The calculation can also be confirmed by scaling to the reported volumes, for example. Using the mid-range 85 kg $\mathrm{FOE/m^3}$ (≈fuel oil at η = 0.35),

$$\text{Annual fuel saved} \approx 85\ \frac{\mathrm{kg}}{\mathrm{m^3}} \times 3{,}000{,}000\ \mathrm{m^3} = 255{,}000\ \mathrm{t\ (FOE)}$$
$$\text{Cross-check via gas: } 35\ \mathrm{m^3\ NG/m^3} \Rightarrow 105\ \text{million}\ \mathrm{m^3\ NG/year\ (avoided)}$$

These two expressions are consistent: 35 $\mathrm{m^3}$ NG per $\mathrm{m^3}$ corresponds to ≈70–85 kg fuel equivalent per $\mathrm{m^3}$ once the same efficiency envelope is applied. Summarizing, the range (70–100 $\mathrm{kg/m^3}$) reflects uncertainties in (i) boiler and distribution efficiency (η), (ii) fuel mix and LHV, and (iii) operational set-points (target temperature, hold time, mold loading). A sensitivity sweep over η = 0.30–0.40 and fuel LHV brackets preserves the 70–100 $\mathrm{kg/m^3}$ interval for FOE.

It should be noted that the calculations presented in this section quantify process-level energy and fuel savings associated with replacing conventional steam curing with THAC-assisted solar curing. The resulting reduction in external fuel demand (expressed in kWh, $\mathrm{m^3}$ of natural gas, or fuel oil equivalent) represents a directly demonstrable reduction in energy use during the curing stage.

While the composite binder applied in this study contains a reduced fraction of Portland cement clinker, the present analysis does not claim a proportional reduction in binder-related CO_2 emissions, as the production of quicklime is also associated with significant process emissions. Accordingly, the reported environmental benefit should be interpreted primarily as a reduction in operational energy demand and fossil fuel consumption during curing, combined with partial substitution of clinker by industrial by-products (ash). A comprehensive life-cycle assessment quantifying net CO_2 effects of clinker–lime substitution is beyond the scope of the present work and is identified as a subject for further investigation.

5. Discussion

The following discussion focuses on the interpretation of results obtained under laboratory-scale and controlled climatic conditions, with emphasis on the mechanisms governing hydration, heat transfer, and early-age hardening.

Laboratory studies have confirmed the effectiveness of concrete based on a composite binder, both with steam curing and with solar thermal treatment using translucent and heat-accumulating coatings (THACs). Sun-curing concrete based on a composite binder with THAC reduces the consumption of clinker by 50% (process-level comparisons) and equivalent fuel during heat–moisture treatment by 70–100 kg per 1 m^3 of concrete (process-level comparisons). The low heat flux during heating of concrete products in a helioform with THAC ensures optimal utilization of the heat of cement hydration (up to 50% of the total thermal energy). The implementation of this new technology improves energy efficiency at all stages of concrete heat treatment.

The environmental benefits observed in this study are directly linked to the applied mix design and the use of a clinker-reduced composite binder. Composite binders incorporating up to 30 wt.% of thermal power plant (TPP) ash enable a dual environmental effect. First, the utilization of TPP ash contributes to the reduction in ash disposal volumes, mitigating the long-term environmental burden associated with ash dumps and land occupation. Second, partial replacement of Portland cement with TPP ash results in a proportional reduction in clinker demand, which is particularly significant given that clinker production remains the most energy-intensive and carbon-intensive stage of cement manufacture.

In the context of the present study, the use of a composite binder containing 30% TPP ash, combined with THAC-assisted solar curing, amplifies these benefits by simultaneously lowering material-related and process-related environmental impacts. The reduced clinker content decreases embodied energy and associated emissions at the material level, while the solar-assisted curing regime further limits external fuel demand during early-age hardening. This synergy between binder design and curing technology provides a quantifiable and mechanism-based justification for the reported reduction in environmental impact, rather than a purely qualitative sustainability claim.

The consolidated evidence from replicated series under controlled hot-arid simulations confirms that THAC curing can be engineered to harvest cement hydration heat as a first-order energy source during the most energy-intensive early stage, with the hydration share approaching ~50% of total heating. Within one experimental framework, THAC delivered rapid early strength, microstructural compactness and frost resistance comparable to normal curing, while avoiding the structural coarsening and performance penalties characteristic of conventional steaming; concurrently, the composite binder with 50% clinker reduction maintained mechanical targets, translating into 70–100 kg lower fuel demand per m^3 of concrete. These results elevate THAC from a qualitative concept to a quantitatively parameterized process option; frame mounting and chamber boundary conditions are explicitly linked to maturity and strength outcomes. Practically, this defines a scalable decarbonization lever for precast operations in solar-rich regions and aggregates-constrained contexts, and motivates future work on:

- Statistical optimization across broader binder chemistries and W/C windows;
- predictive control using maturity-based cure scheduling;
- pilot-scale retrofits at the plant level to validate throughput and cost models under real-world variability.

Taking into consideration the mechanistic interpretation, it should be stressed that the THAC establishes a moisture-retentive, low-intensity boundary condition that mitigates evaporative cooling and sustains a near-saturated interlayer, while providing a modest radiative/convective input. Under these conditions, the thermal history shows accelerated maturity at low gradients, consistent with sustained NG→I stages in the Krstulović–Dabić framework rather than prematurely diffusion-limited growth [44,45]. The synergy between solar input and hydration heat explains the rapid early strength without the microstructural coarsening sometimes reported for steam cycles when not optimized [46]. Within one

experimental framework, our side-by-side data (THAC vs. steam vs. normal) therefore align with current thermo-hygro-chemical models of early-age heat–moisture transport and with maturity practice, supporting THAC as a quantitatively parameterized, energy-lean route to accelerated hardening [47–49].

The proposed solution has also been compared with some alternatives, taking into consideration the information presented in the literature, in Table 8.

Table 8. Literature comparison for the main features of the THAC solution.

Aspect	THAC—This Study	Steam Curing [47,48,50,51]	Modeling & Kinetics Anchors [49,52]
Boundary condition and flux	Low-intensity solar/radiative input with a narrow, moisture-retentive interlayer → soft thermal gradients; maturity rises while hydration heat provides a substantial fraction of the early input.	High external flux can impose steep gradients and moisture redistribution unless regimes are optimized and/or supported by SCMs and secondary curing; later-age transport can be sensitive to the chosen regime.	Thermo-hygro-chemical (THC) and heat–moisture coupling models; maturity (ASTM C1074) formalizes temperature–time effects.
Early-age strength and maturity	Fast early strength with rising maturity at low gradients; side-by-side superiority vs. normal curing in the first 1–2 days.	Strong early strength is typical; however, the benefit depends on the cycle and materials; optimization is often required for long-term properties.	Maturity method (Nurse–Saul/Arrhenius) and early-age thermal modeling for prediction and scheduling.
Microstructure and durability	Microstructure and frost resistance comparable to normal curing; avoids some coarsening effects reported under harsher steam cycles.	Reviews and recent studies report potential later-age penalties (e.g., transport, carbonation) for some steam regimes unless optimized or SCM-assisted; supplementary curing can mitigate.	Models linking local T/RH to hydration degree and pore structure evolution; kinetic partitioning NG/I/D.
Energy and process implications	Energy-lean route (low external flux) with substantial utilization of hydration heat; compatible with clinker-reduced binders.	Higher process energy; can be mitigated by optimized cycles and SCMs, but still externally energy-intensive.	Hybrid data-and-physics temperature prediction; maturity/degree-hours as operational KPI.

The findings of this study hold significant promise for industrial-scale applications in precast concrete production, particularly in regions with abundant solar resources like Central Asia or arid zones. For the regions of the Republic of Kazakhstan, where there is a shortage of coarse aggregate, the use of fine-grained concretes on fine sands is of great importance. Compositional binder in combination with concrete heliotechnology seems to be promising. Solar thermal treatment using composite binders and THACs enables manufacturers to produce high-quality concrete elements—such as slabs, beams, and panels—for construction projects while slashing energy costs by 70–100 kg of fuel per m^3. This method is especially viable for prefabricated housing, infrastructure (bridges, culverts), and modular buildings, where accelerated hardening reduces production cycles from days to hours.

The effectiveness of solar thermal treatment of concrete using a composite binder in helioform with a THAC allows for the use of solar heat as an additional energy source, which will reduce the need for heating systems and energy consumption, improving the

environmental friendliness of production. The conception of applying this solution in production is presented in Figure 3.

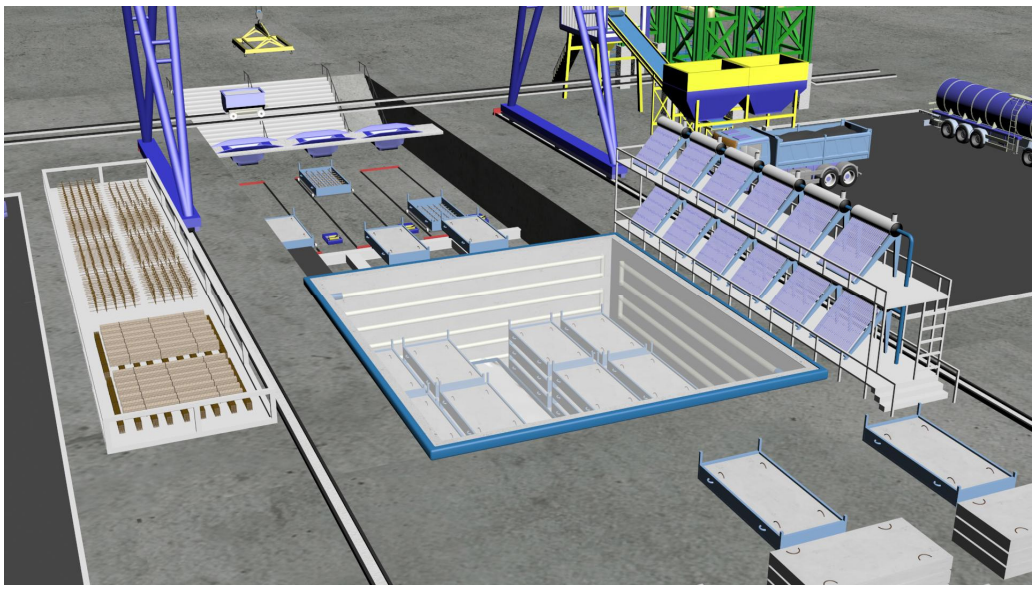


Figure 3. Conceptual scheme of THAC-assisted solar curing integrated into the precast concrete production process.

Figure 3 situates THAC within the manufacturing line and clarifies how the boundary condition (moisture-retentive, low-intensity radiative input) stabilizes heat–moisture transfer at an early age. The scheme illustrates the production sequence from fresh mix casting to demolding under hybrid curing conditions. After placement in standard steel molds, a THAC insert establishes a narrow, moisture-retentive interlayer above the concrete surface. During daytime, incident solar radiation is partially transmitted and trapped by THAC, while the concrete acts as an absorber/thermal mass; at night, the same interlayer limits convective and evaporative losses, enabling "thermos-like" heat retention. The moderated flux maintains a soft thermal gradient, supports near-saturated air in the interlayer, and allows early-age hydration heat to supply a significant share of the total energy input.

In addition to the positive environmental impacts, the use of renewable energy makes it possible to focus on solar concrete technology in the southern regions of Kazakhstan. Reducing the clinker content of the composite binder by up to 50% and reducing fuel consumption by 70–100 kg per 1 m^3 of concrete using solar thermal treatment has significant positive consequences, significantly improving the environmental, energy, and economic sustainability of concrete production, and is an important area for the sustainable development of the construction industry. Rational use of intense solar heating and the conservation of the internal heat from the exothermic effect of the composite binder when using helioforms with THAC improve the energy efficiency, process stability, and quality of reinforced concrete products (Figure 4).

Figure 4 explains how solar energy is operationally integrated with conventional resources under a single control envelope. Thus, solar thermal treatment of concrete using a composite binder in helioforms with THAC is a new technological approach aimed at improving the energy efficiency of production. This conception allows for energy and control flows between (i) the solar input harvested through THAC, (ii) optional auxiliary heat (e.g., low-load gas boiler or electric IR), and (iii) process control (temperature, humidity, and maturity). The controller prioritizes solar-derived heat and hydration heat, invoking auxiliary input only to maintain set-points (e.g., cap temperature, maturity index) during adverse weather or off-peak irradiance. Measured variables include concrete core/surface

temperature, interlayer relative humidity, and solar irradiance; manipulated variables include shuttering/vent settings, auxiliary heater duty, and cycle duration.

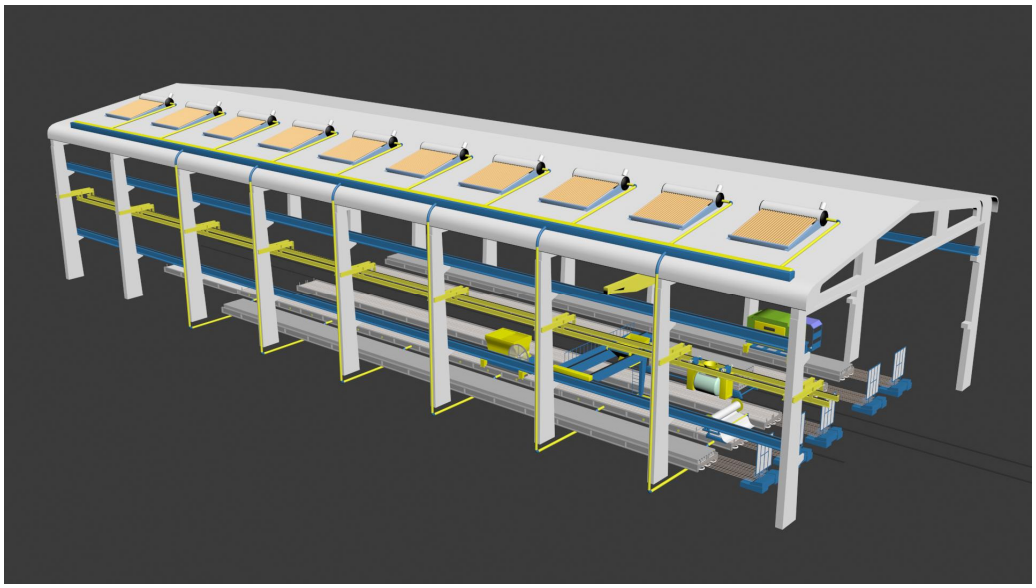


Figure 4. Conceptual scheme of a hybrid energy supply concept for concrete curing combining solar and conventional energy sources.

Based on the literature data, it is worth noting that presented technology is connected with certain limitations, including non-uniform temperature fields and early-age cracking under intense solar radiation, increased evaporation and plastic shrinkage, as well as the need for strict control of moisture retention in solar [36,37]. These limitations confirm that stable hydration conditions under solar energy require dedicated thermal–moisture control systems, such as THAC, to mitigate risks of drying, surface cracking, and excessive temperature gradients.

Key applications extend to remote or off-grid facilities, where reliance on fossil fuels for steaming is impractical. By halving clinker content (50% reduction), the approach supports low-carbon cement plants, aligning with circular economy principles, including EU Green Deal targets [1,2]. Pilot implementations could target small-to-medium enterprises producing agro-storage silos or water reservoirs, leveraging natural hydration optimization for durable, steam-free products comparable to traditionally cured concrete. In this case, additional research connected with the durability of the material and leachability in specific conditions will be required. Future applications and research directions can also include 3D-printed concrete elements and retrofitting existing plants with solar THAC systems, potentially cutting global cement emissions by promoting widespread adoption in developing markets. The proper regulation of hardening is one of the key problems in 3D printing applications of cementitious materials [1,53,54].

From a broader perspective, the results of this study have clear implications for both policy frameworks and industrial practice in the context of sustainable construction. The demonstrated reduction in clinker demand and external energy consumption supports ongoing efforts to decarbonize the cement and concrete sector and aligns with emerging low-carbon building regulations and climate targets [55,56]. For precast concrete producers, THAC-assisted solar curing offers a viable pathway for reducing reliance on fossil-fuel-based steam curing, particularly in solar-rich regions, while maintaining process reliability and product quality. The findings may inform future updates of curing guidelines, factory energy benchmarks, and incentive schemes promoting renewable energy integration in construction materials manufacturing. In this sense, the proposed approach contributes not

only as a technological solution but also as a practical enabler for policy-driven transitions toward energy-efficient and climate-resilient concrete production [6,18].

6. Conclusions

The results of this study confirm that, under laboratory-scale conditions, concretes based on the investigated composite binder can be effectively hardened using accelerated curing techniques, including both conventional steam curing and THAC-assisted solar curing. The conclusions drawn are limited to the tested materials, curing configurations, and controlled experimental environment.

The laboratory experiments demonstrated that the applied composite binder formulation enables a 50% reduction in the clinker fraction of the binder, while maintaining mechanical performance and microstructural characteristics comparable to those of normally cured concretes at the age of 28 days. When combined with THAC-assisted solar heat treatment, this binder system allowed a substantial reduction in external energy demand during early-age curing. Based on process-level estimates, the equivalent fuel consumption during heat and moisture treatment was reduced by approximately 70–100 kg per 1 m^3 of concrete, relative to conventional steam curing.

The low intensity of the solar heat flux characteristic of THAC-based curing differs fundamentally from high-intensity steam regimes. Under the investigated conditions, this moderated thermal input enabled effective utilization of cement hydration heat, which contributed up to approximately 50% of the total energy absorbed during the heating stage, as reflected in the measured temperature development and maturity index. This mechanism supports accelerated hardening without imposing steep thermal gradients typically associated with traditional steaming.

Within the scope of the present laboratory investigation, the use of helioforms with THACs represents a feasible accelerated curing concept in which external thermal input primarily enhances the utilization of internally generated hydration heat during the most energy-intensive stage of hardening. While the results indicate potential relevance for future industrial application, full-scale implementation requires further validation at pilot and industrial scales, including long-term durability assessment and evaluation under variable climatic and production conditions.

Author Contributions: Conceptualization, A.U. and L.A.; methodology, L.A. and A.J.; validation, K.K. and K.B.; formal analysis, K.K.; investigation, A.U.; resources, L.A. and A.J.; data curation, A.U. and K.B.; writing—original draft preparation, A.U., L.A. and K.K.; writing—review and editing, K.B. and A.J.; visualization, A.U.; supervision, L.A. and A.J.; project administration, A.J.; funding acquisition, A.J. All authors have read and agreed to the published version of the manuscript.

Funding: This research has been funded by the Committee of Science of the Ministry of Science and Higher Education of the Republic of Kazakhstan, Grant No. BR21882278, entitled: "Establishment of a construction and technical engineering centre to provide a full cycle of accredited services to the construction, road-building sector of the Republic of Kazakhstan".

Data Availability Statement: The original contributions presented in this study are included in the article. Further inquiries can be directed to the corresponding author.

Acknowledgments: During the preparation of this manuscript, the authors used Grammarly (v1.2.220.1800) for the purposes of English correction.

Conflicts of Interest: The authors declare no conflicts of interest. The funders had no role in the design of the study; in the collection, analyses, or interpretation of data; in the writing of the manuscript; or in the decision to publish the results.

Abbreviations

The following abbreviations are used in this manuscript:

NG	Natural gas
THAC	Translucent heat-accumulating coating
PVC	Polyvinyl chloride

References

1. Korniejenko, K.; Mikuła, J.; Brudny, K.; Aruova, L.; Zhakanov, A.; Jexembayeva, A.; Zhaksylykova, L. A Review of Industrial By-Product Utilization and Future Pathways of Circular Economy: Geopolymers as Modern Materials for Sustainable Building. *Sustainability* **2025**, *17*, 4536. [CrossRef]
2. Althoey, F.; Ansari, W.S.; Sufian, M.; Deifalla, A.F. Advancements in Low-Carbon Concrete as a Construction Material for the Sustainable Built Environment. *Dev. Built Environ.* **2023**, *16*, 100284. [CrossRef]
3. Kumar, A.; Kumar, P.; Gogineni, A.; Ahmed, M.; Chen, W. Evolution of Cementitious Binders: Overview of History, Environmental Impacts, and Emerging Low-Carbon Alternatives. *Buildings* **2025**, *15*, 3811. [CrossRef]
4. Chen, H.; Li, N.; Unluer, C.; Chen, P.; Zhang, Z. 200 Years of Portland Cement: Technological Advancements and Sustainability Challenges. *J. Clean. Prod.* **2025**, *486*, 144500. [CrossRef]
5. Future Market Insights. Building Materials Market Building. Available online: https://www.futuremarketinsights.com/reports/building-materials-market (accessed on 27 December 2025).
6. Haigh, R.; Ameri Sianaki, O. Traditional and Advanced Curing Strategies for Concrete Materials: A Systematic Review of Mechanical Performance, Sustainability, and Future Directions. *Appl. Sci.* **2025**, *15*, 11055. [CrossRef]
7. Pawar, Y.; Kate, S.R. Curing of Concrete: A Review. *Int. Res. J. Eng. Technol.* **2020**, *7*, 1820–1824.
8. Ozer, N.; Ozgünler, S.A.; Ozdamar, S. Investigation of Production Possibilities of Natural Hydraulic Binders from Marls. *Constr. Build. Mater.* **2025**, *489*, 140675. [CrossRef]
9. Aruova, L.B.; Aruova, A.B.; Shashpan, Z.A.; Utkelbaeva, A.O.; Alibekov, N.B. Manufacturing Arbolitic Building Products Using Solar Energy. *J. Mech. Eng. Res. Dev.* **2018**, *41*, 49–55. [CrossRef]
10. Lyazat, A. Process Parameters of Production of Non-Autoclaved Aerated Concrete on the Basis of Complex Use of Ash and Gypsum-Containing Wastes. *Mediterr. J. Soc. Sci.* **2014**, *5*, 2565–2571. [CrossRef]
11. Tokmyrza, B.; Aruova, L.; Dauzhanov, N.; Ospanova, Z.; Utkelbaeva, A. Comprehensive Heat Treatment Using Solar Energy to Produce High Quality Foam Concrete. *E3S Web Conf.* **2019**, *116*, 00092. [CrossRef]
12. Kuatbayeva, T.K.; Zhambakina, Z.M.; Yespayeva, A.S.; Zhakapbayeva, G.A. Research of Technological Properties of the Composition of Binding Binders, Modified with Waste of Processing of Petroleum Bituminous Rocks. *J. Phys. Conf. Ser.* **2021**, *1926*, 012031. [CrossRef]
13. Sathya Narayanan, J.; Ramamurthy, K. Development of Solid, Foam Concrete Interlocking Blocks and Studies on Short Masonry Specimen. *Mason. Int.* **2013**, *26*, 7–16.
14. Namsone, E.; Šahmenko, G.; Korjakins, A. Durability Properties of High Performance Foamed Concrete. *Procedia Eng.* **2017**, *172*, 760–767. [CrossRef]
15. Cease, M.E.; White, D.H. Emulsification of Thermal Energy Storage Materials in an Immiscible Fluid. *Int. J. Energy Res.* **1983**, *7*, 109–119. [CrossRef]
16. Kuz'min, M.P.; Larionov, L.M.; Kondratiev, V.V.; Kuz'mina, M.Y.; Grigoriev, V.G.; Kuz'mina, A.S. Use of the Burnt Rock of Coal Deposits Slag Heaps in the Concrete Products Manufacturing. *Constr. Build. Mater.* **2018**, *179*, 117–124. [CrossRef]
17. Kuz'min, M.; Larionov, L.; Kuz'mina, M.; Kuz'mina, A.; Ran, J.; Burdonov, A.; Zenkov, E. Production of Portland Cement Using Fluorine Gypsum—Hydrofluoric Acid Waste. *Mag. Civ. Eng.* **2022**, *111*, 11113. [CrossRef]
18. Boudjemaa, T.; Hamid, K.; Nabil, B.; Saïd, B.; Khelifa, L.; Mohammed, B.; Dine, H.D.N.; Abdeldjalil, S.; Abdeldjalil, D. Solar Energy-Driven Heat Treatment of Concrete and Mortar in Desert Environments: A Case Study of Bechar Region, Algeria. *Res. Eng. Struct. Mat.* **2025**, *11*, 3133–3148. [CrossRef]
19. Penjiyev, A.M. Wave Energy Resources of the Caspian Sea on the Coast of Turkmenistan. *Appl. Sol. Energy* **2022**, *58*, 306–310. [CrossRef]
20. Zakhidov, R.A.; Tajiyev, U.A.; Kiseleva, E.I.; Yusupov, D.T.; Yusupov, D.T.; Saliev, G.S.; Gorobtsov, S.I. On the Possibility of Sustainable Energy and Water Supply of Low-Rise Residential Buildings Located in Areas with an Arid Climate Using Combined Wind and Solar Photovoltaic Power Complexes of Low Power. *Appl. Sol. Energy* **2022**, *58*, 159–164. [CrossRef]
21. Aimenov, A.; Aimenov, Z. Influence of Heliothermal Treatment on Physical and Technical Characteristics of Concretes. In Proceedings of the VIII International Annual Conference "Industrial Technologies and Engineering" (ICITE 2021), Shymkent, Kazakhstan, 11–12 November 2021; p. 020004.

22. Ibragimov, A.M.; Aksakovskaya, L.N.; Gerasimova, S.V. Mathematical Model for Heat and Mass Transfer of Concrete Heat Treatment Using Solar Power. *Light Eng.* **2023**, *31*, 12–21. [CrossRef]
23. Ibragimov, A.M.; Gnedina, L.Y.; Gerasimova, S.V. The Usage of Solar Power in the Heating Treatment of Concrete. *Light Eng.* **2021**, *29*, 44–50. [CrossRef]
24. Benammar, B.; Mezghiche, B.; Guettala, S. Influence of Atmospheric Steam Curing by Solar Energy on the Compressive and Flexural Strength of Concretes. *Constr. Build. Mater.* **2013**, *49*, 511–518. [CrossRef]
25. Singh, A.P.; Tiwari, S.; Sinhmar, H.; Sahdev, R.K.; Tripathi, S. Enhancing Solar Drying Performance with Heat Storage Technologies and Nanoparticles Integration: A Clean Energy Production. *J. Energy Storage* **2025**, *105*, 114669. [CrossRef]
26. Olsson, J.A.; Miller, S.A.; Kneifel, J.D. A Review of Current Practice for Life Cycle Assessment of Cement and Concrete. *Resour. Conserv. Recycl.* **2024**, *206*, 107619. [CrossRef]
27. Shahalami, S.M.; Ahmadnia, S.; Armanfard, S.; Kamali, A.R. Locating Electric Vehicle Solar Charging and Discharging Stations Using Multi-Objective Genetic Algorithm and Fuzzy Decision Making. *Appl. Sol. Energy* **2022**, *58*, 177–186. [CrossRef]
28. Klychev, S.I.; Rasakhodzhaev, B.S.; Akhadov, Z.Z.; Akhmadjonov, U.Z.; Adylov, C.A. Study of the Thermal Regime of Solar Greenhouses for the Individual Purpose for Their Design Features. *Appl. Sol. Energy* **2022**, *58*, 121–126. [CrossRef]
29. Mugahed Amran, Y.H.; Rashid, R.S.M.; Hejazi, F.; Abang Ali, A.A.; Safiee, N.A.; Bida, S.M. Structural Performance of Precast Foamed Concrete Sandwich Panel Subjected to Axial Load. *KSCE J. Civ. Eng.* **2018**, *22*, 1179–1192. [CrossRef]
30. Muthu Kumar, E.; Ramamurthy, K. Effect of Fineness and Dosage of Aluminium Powder on the Properties of Moist-Cured Aerated Concrete. *Constr. Build. Mater.* **2015**, *95*, 486–496. [CrossRef]
31. Hu, C.; Li, H.; Liu, Z.; Wang, Q. Research on Properties of Foamed Concrete Reinforced with Small Sized Glazed Hollow Beads. *Adv. Mater. Sci. Eng.* **2016**, *2016*, 5820870. [CrossRef]
32. Kearsley, E.P.; Wainwright, P.J. Ash Content for Optimum Strength of Foamed Concrete. *Cem. Concr. Res.* **2002**, *32*, 241–246. [CrossRef]
33. Ali, M.A.; Ahmed, H.U. Influence of Various Curing Conditions on the Mechanical, Durability, and Microstructural Properties of Concrete: A Comprehensive Review. *Innov. Infrastruct. Solut.* **2026**, *11*, 25. [CrossRef]
34. Thissen, P.; Bogner, A.; Dehn, F. Surface Treatments on Concrete: An Overview on Organic, Inorganic and Nano-Based Coatings and an Outlook about Surface Modification by Rare-Earth Oxides. *RSC Sustain.* **2024**, *2*, 2092–2124. [CrossRef]
35. Zheng, L.; Xiong, T.; Shah, K.W. Transparent Nanomaterial-Based Solar Cool Coatings: Synthesis, Morphologies and Applications. *Sol. Energy* **2019**, *193*, 837–858. [CrossRef]
36. Liang, Z.; Zhou, H.; Zhao, C.; Wang, F.; Zhou, Y. Experimental and Numerical Study of the Influence of Solar Radiation on the Surface Temperature Field of Low-Heat Concrete in a Pouring Block. *Buildings* **2023**, *13*, 1519. [CrossRef]
37. Moelich, G.M.; Van Zyl, J.E.; Rabie, N.; Combrinck, R. The Influence of Solar Radiation on Plastic Shrinkage Cracking in Concrete. *Cem. Concr. Compos.* **2021**, *123*, 104182. [CrossRef]
38. *GOST 18105-2018*; Concrete Rules for Control and Strength Assessment. GOST R: Moscow, Russia, 2019.
39. *GOST 10060-2012*; Methods for the Determination of Frost-Resistance. GOST R: Moscow, Russia, 2012.
40. Aruova, L.; Tolkynbaev, T.; Kirgizbaev, A.; Aruov, B.; Kalieva, Z.; Gordienko, B.; Nurbayeva, M. Solar Energy for Foam Concrete Production Technology in Modern Conditions. *Appl. Sol. Energy* **2022**, *58*, 854–859. [CrossRef]
41. Higher Calorific Values of Common Fuels: Reference & Data. Available online: https://www.engineeringtoolbox.com/fuels-higher-calorific-values-d_169.html (accessed on 3 March 2026).
42. Energy Supply Systems for Buildings. Available online: https://ocw.tudelft.nl/wp-content/uploads/Summary_table_with_heating_values_and_CO2_emissions.pdf (accessed on 3 March 2026).
43. Typical Calorific Values of Fuel. Available online: https://www.forestresearch.gov.uk/tools-and-resources/fthr/biomass-energy-resources/reference-biomass/facts-figures/typical-calorific-values-of-fuels/ (accessed on 3 March 2026).
44. Wu, C.-R.; Xiao, Z.-P.; Wei, J.-J.; Kou, S.-C.; Tang, M.-X. Early Hydration Behaviours and Kinetics of Portland Cement Composites Incorporating Low-Calcium Circulating Fluidized Bed Fly Ash. *J. Compos. Sci.* **2025**, *9*, 671. [CrossRef]
45. Duan, Z.; Li, J.; Zou, S.; Huang, T.; Li, B.; Hu, Z.; Li, L. Hydration Kinetics and Modified Model for Effective Water to Cement Ratio Control in Recycled Aggregate Concrete. *Case Stud. Constr. Mater.* **2025**, *23*, e05217. [CrossRef]
46. Dinh Thien, B.; Vinh Long, H. A Study of Using Solar Energy to Cure Concrete Bricks. *E3S Web Conf.* **2019**, *97*, 06041. [CrossRef]
47. Al-Sodani, K.A.A. Production, Thermal, Durability, and Mechanical Properties of Translucent Concrete and Its Applications in Sustainable Construction: A Review. *Buildings* **2025**, *15*, 3314. [CrossRef]
48. Sáez Del Bosque, I.F.; Martínez-Ramírez, S.; Martín-Pastor, M.; Blanco-Varela, M.T. Effect of Temperature on C–S–H Gel Nanostructure in White Cement. *Mater. Struct.* **2014**, *47*, 1867–1878. [CrossRef]
49. Sharifi, S.; Navabi, D.; Mosavi, A. Translucent Concrete: Comprehensive Review of Concepts, Recent Technologies and Advances in Light Transmitting Concrete. In Proceedings of the 2023 IEEE 17th International Symposium on Applied Computational Intelligence and Informatics (SACI), Timisoara, Romania, 23–26 May 2023; pp. 000685–000692.

50. Al-saffar, F.Y.; Wong, L.S.; Paul, S.C. An Elucidative Review of the Nanomaterial Effect on the Durability and Calcium-Silicate-Hydrate (C-S-H) Gel Development of Concrete. *Gels* **2023**, *9*, 613. [CrossRef]
51. Al-Gburi, M.; Abed, J.; Almssad, A.; Alhayani, A.A.; Jędrzejewska, A.; Nilsson, M. The Effect of Real Curing Temperatures on Early Age Concrete Strength Development in Massive Concrete Structures. *Eur. J. Environ. Civ. Eng.* **2025**, *29*, 1832–1847. [CrossRef]
52. Ahmed, S.; El-Tair, A.M.; Rabeeh, B.M. Sustainable, Self-Cured Concrete toward a Thermally and Radiation Shielding Concrete. *Innov. Infrastruct. Solut.* **2024**, *9*, 198. [CrossRef]
53. Baigarina, A.; Shehab, E.; Ali, M.H. Construction 3D Printing: A Critical Review and Future Research Directions. *Prog. Addit. Manuf.* **2023**, *8*, 1393–1421. [CrossRef]
54. Mierzwiński, D.; Łach, M.; Gądek, S.; Lin, W.-T.; Tran, D.H.; Korniejenko, K. A Brief Overview of the Use of Additive Manufacturing of Con-Create Materials in Construction. *Acta Innov.* **2023**, *48*, 22–37. [CrossRef]
55. Marandi, N.; Shirzad, S. Sustainable Cement and Concrete Technologies: A Review of Materials and Processes for Carbon Reduction. *Innov. Infrastruct. Solut.* **2025**, *10*, 408. [CrossRef]
56. Griffiths, S.; Sovacool, B.K.; Furszyfer Del Rio, D.D.; Foley, A.M.; Bazilian, M.D.; Kim, J.; Uratani, J.M. Decarbonizing the Cement and Concrete Industry: A Systematic Review of Socio-Technical Systems, Technological Innovations, and Policy Options. *Renew. Sustain. Energy Rev.* **2023**, *180*, 113291. [CrossRef]

Disclaimer/Publisher's Note: The statements, opinions and data contained in all publications are solely those of the individual author(s) and contributor(s) and not of MDPI and/or the editor(s). MDPI and/or the editor(s) disclaim responsibility for any injury to people or property resulting from any ideas, methods, instructions or products referred to in the content.